Bulletin of the Earthquake
Research Institute
Vol. 48 (1970), pp. 171-188

12. *Vertical Crustal Deformation and Tsunami Energy.*

By Tokutaro HATORI,

Earthquake Research Institute.

(Read Oct. 28, 1969.—Received Jan. 31, 1970.)

Abstract

Since the tsunami is closely related to vertical crustal movement at the time of earthquake occurrence, the vertical crustal movements surveyed on land and in the sea are reviewed. From the data, the total volume of displaced material and the potential energy of imaginary tsunami are calculated. The energy obtained for imaginary tsunamis is compared with the tsunami energy calculated from tsunami waves, in relation to earthquake magnitude. There is discrepancy of energy value for the same magnitude of earthquake, but whether this discrepancy is real or not is not known at present.

1. Introduction

From amplitudes and periods of the tsunami waves observed at the coast near the tsunami source, Takahasi (1951) inferred the tsunami energy in the case of the 1933 Sanriku tsunami. Since then, the tsunami energy for various earthquakes was calculated by many investigators based on records observed by tide gauge. However, the calculated values given by different investigators varied considerably. In the present paper, the potential energies are calculated for the imaginary tsunami corresponding to the vertical displacement of the ground caused by land earthquake. The tsunami energy obtained from both methods is investigated in relation to earthquake magnitude.

In the cases of the 1923 Kanto, 1935 Taiwan and 1964 Alaska earthquakes, the features of crustal deformation have been indicated by the contour lines. Iida (Ishimoto, 1937) and Miyoshi (1968) calculated the volume of displaced material in the regions of land and sea, respectively, for the Kanto earthquake. As for other earthquakes (Tango of 1927, Tottori of 1943, Fukui of 1948, etc.), the contour lines of crustal deformation are drawn with the aid of the results of leveling and triangulation surveys. Making use of a planimeter, the displaced volumes caused by earthquake are measured. For several earthquakes, the volume of upheaval compares favorably with that of subsidence.

2. Data of vertical crustal movement

The earthquake data used in analysis are given in Table 1. The contour maps of crustal movement accompanying those earthquakes are shown in the following figures, where closed circles represent bench marks

Table 1. Land and submarine earthquakes accompanied by crustal deformation.

Date	Epicenter		Location	Depth (km)	*M*	Remark
	Lat. N	Long. E				
1923 Sept. 1	35.3°	139.3°	Kanto	Shallow	7.9	Tsunami
1927 Mar. 7	35.6	135.1	Tango	10	7.5	Tsunami
1935 Apr. 21	24.3	120.6	Taiwan	5	7.1	Land earthq.
1939 May 1	40.0	139.8	Oga	0	7.0	Tsunami
1943 Sept. 10	35.5	134.2	Tottori	10	7.4	Land earthq.
1945 Jan. 13	34.7	137.0	Mikawa	0	7.1	Tsunami
1948 June 28	36.1	136.2	Fukui	20	7.3	Land earthq.
1964 Mar. 28	61.1N	147.7W	Alaska	20-50	8.4	Tsunami
1964 June 16	38.4	139.2	Niigata	40	7.5	Tsunami

on leveling route and the visual points along the coast, and open circles the triangulation points. The contour lines are drawn, based on the measured points. The contours of upheaval and subsidence are indicated by a solid or broken line respectively.

1) The Kanto earthquake of 1923

This is a famous earthquake, when the capes of Boso and Miura Peninsula were upheaved about 1.5 m. Leveling and triangulation surveys were carried out by the Military Land Survey, the contour lines (Matuzawa, 1964) being reproduced in Fig. 1. The topographic change of the sea bottom in Sagami Bay was surveyed by the Hydrographic Office of Japan. Abnormal topographic change of more than 100 m was discussed by Mogi (1959), Hatori (1966) and Aida (1969). The tsunami source area inferred from an inverse refraction diagram is indicated by broken lines in Fig. 1.

2) The Tango earthquake of 1927

Figure 2 shows the contour map of the crustal movement. The contour lines on land are drawn at 10 cm intervals based on the leveling survey (Military Land Survey, 1927) and visual observation (Tanakadate, 1927). The sounding were carried out in 1925 and 1927 by the Hydrographic Office, the contour lines being drawn at 1 m intervals. The

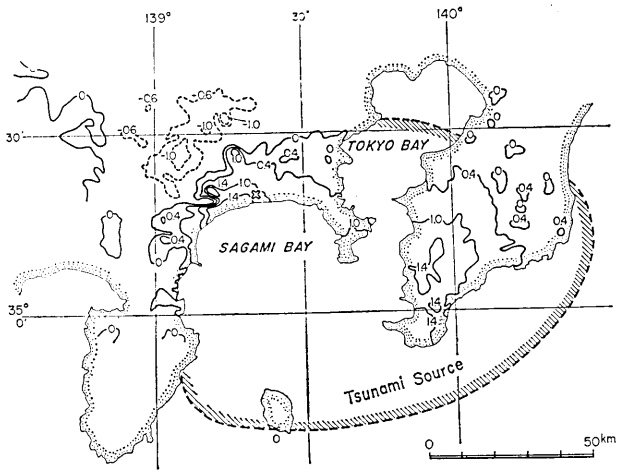

Fig. 1. Contours of upheaval (solid line) and subsidence (broken line) on land, in meters, (after T. Matuzawa) and the estimated source area of tsunami for the 1923 Kanto earthquake.

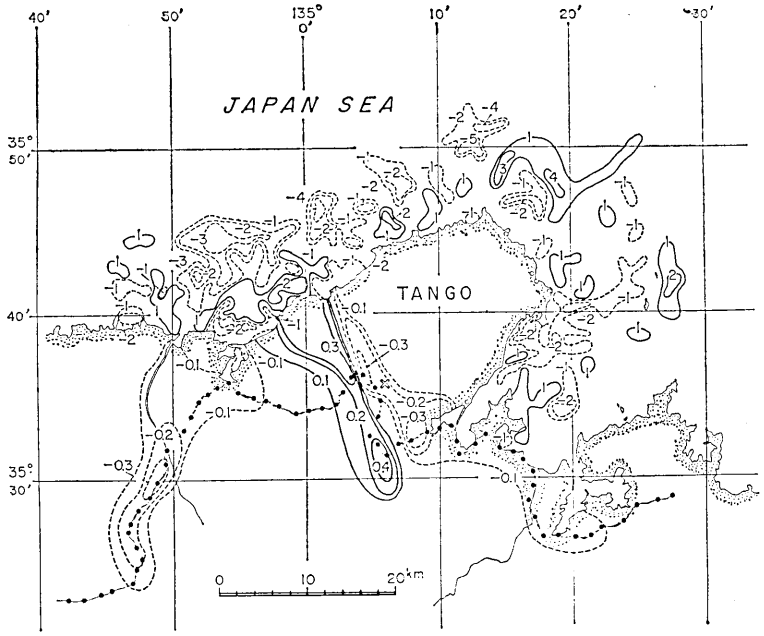

Fig. 2. Contours of upheaval (solid line) and subsidence (broken line) on land and sea bottom, in meters, for the 1927 Tango earthquake.

regions of upheaval and subsidence are divided by a fault line and the maximum displacement is ± 30 cm. The topographic change of the sea bottom being -4 m$\sim$5 m is complex but the fault line on land extends into the sea bed. Accompanying this earthquake, the tsunami was ob-

served by a tide gauge at Tsuiyama. About 1.2 m of tsunami heights was reported around Tango Peninsula as shown in Fig. 3 (Tanakadate, 1927).

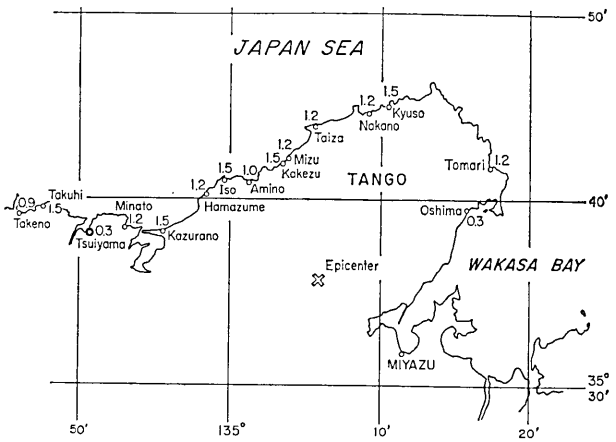

Fig. 3. Distribution of tsunami heights, in meters, for the 1927 Tango earthquake.

3) The Taiwan earthquake of 1935

By the Military Land Survey (1937), the contour map was drawn from the results of leveling and triangulation surveys (Fig. 4). The displacement is in the range of $-1.2\,\mathrm{m} \sim 1.0\,\mathrm{m}$ and the pattern of movement is complex.

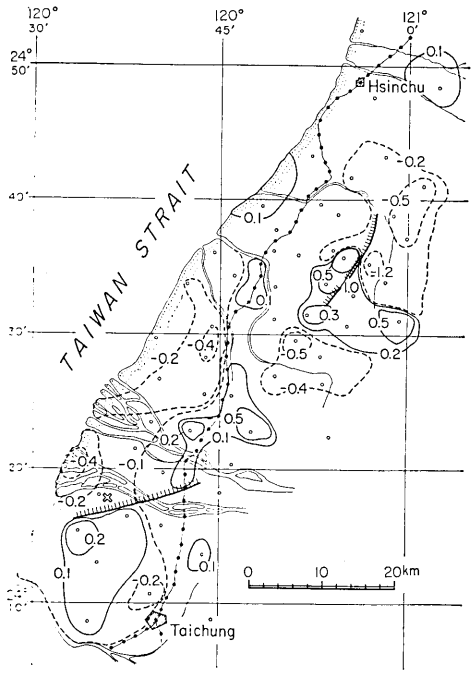

Fig. 4. Contours of upheaval (solid line) and subsidence (broken line), in meters, for the 1935 Taiwan earthquake (after Military Land Survey).

4) The Oga earthquake of 1939

From the results of leveling and triangulation surveys (Imamura, 1944), the contour lines of crustal movement are drawn (Fig. 5). Amount of upheaval increases toward the cape of the peninsula and the maximum displacement is 40 cm. The small tsunami was observed and began with an upward motion at three tide stations (Kishinouye and Iida, 1939). The source area of tsunami inferred from an inverse refraction diagram lies around Oga Peninsula as shown

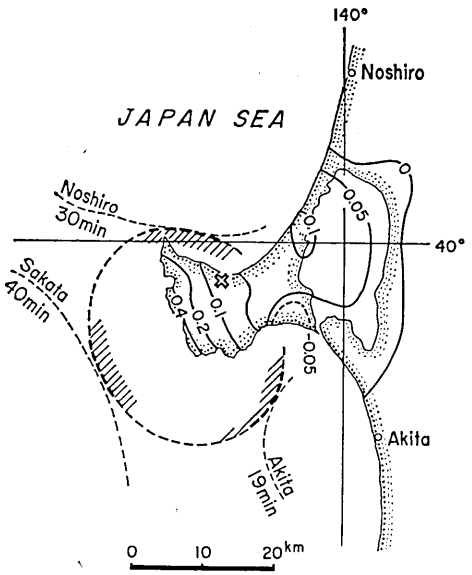

Fig. 5. Contours of vertical crustal deformation, in meters, and the tsunami source area inferred from an inverse refraction diagram for the 1939 Oga earthquake.

in Fig. 5.

5) The Tottori earthquake of 1943

From the result of leveling survey (Military Land Survey, 1944), the contour lines of crustal movement are drawn at 2 cm intervals (Fig. 6). The subsided region along the coast is larger than the upheaved area, and the maximum displacement is −18 cm. Although the tsunami

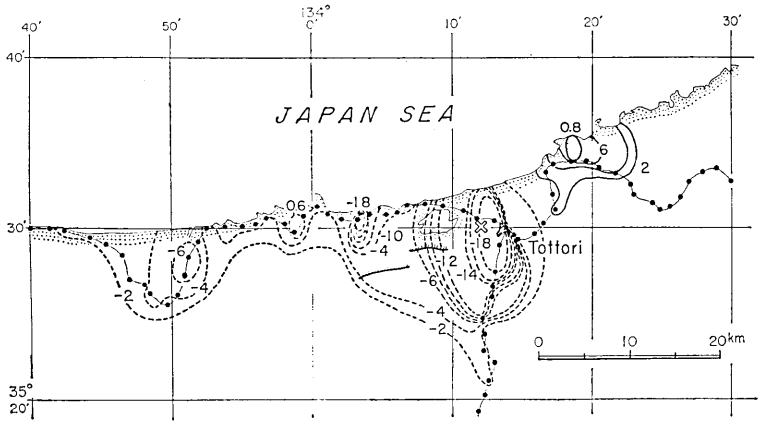

Fig. 6. Contours of upheaval (solid line) and subsidence (broken line), in centimeters, for the 1943 Tottori earthquake.

was not observed, a topographic change of the sea bottom might have occurred.

6) The Mikawa earthquake of 1945

Figure 7 is the compiled contour map of the crustal movement in the regions of land and sea, given by Dambara (1966) and Tayama (1949), respectively. It is seen that the contour lines of upheaval on land continue into Mikawa Bay. According to tide gauge records (Inoue, 1950), the initial motion of tsunami began with a downward motion at Nishiura and upward at Sengen at the time of earthquake occurrence. The sense of the sea level disturbance agreed with the results of the survey. Making use of the records observed in the bay, the source area of the tsunami is inferred by an inverse refraction diagram as shown in Fig. 8. The source area is located in the region of the sea bed change. Fig. 8 also shows the distribution of the maximum wave,

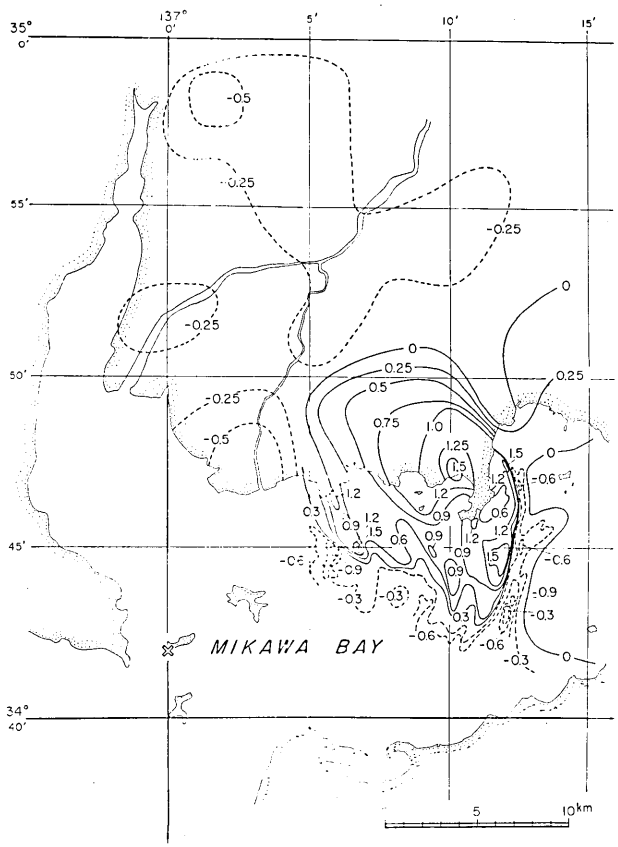

Fig. 7. Contours of upheaval (solid line) and subsidence (broken line) on land (after T. Dambara) and sea bottom (after R. Tayama), in meters, for the 1945 Mikawa earthquake.

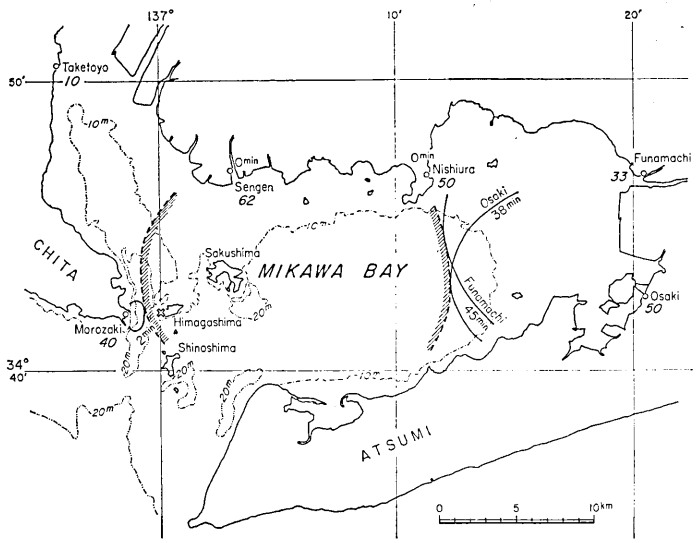

Fig. 8. The tsunami source area inferred from an inverse refraction diagram and distribution of double amplitude of the maximum wave (cm) for the 1945 Mikawa earthquake.

having double amplitudes of 40 cm ~60 cm with short periods.

7) *The Fukui earthquake of 1948*

From the results of leveling and triangulation surveys (Nasu and Rikitake, 1950), the contour lines of crustal movements are drawn at 20 cm intervals (Fig. 9). The range of displacement is −80 cm~40 cm, and the regions of upheaval and subsidence are clearly divided by a fault line directed in NNW-SSE.

8) *The Niigata and Alaska earthquakes of 1964*

Figures 10 and 11 show contour maps of crustal movement given by Plafker (1965) and Mogi *et al* (1964), respectively. In the case of the Alaska earthquake, the upheaved region is located off the shore and the amount of upheaval of more than 8 m was

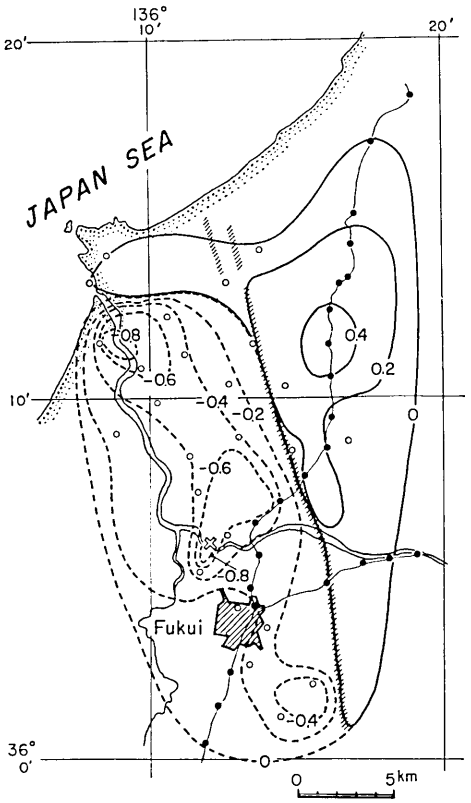

Fig. 9. Contours of upheaval (solid line) and subsidence (broken line), in meters, for the 1948 Fukui earthquake.

surveyed at Montague Island. According to Pararas-Carayannis (1967), the source area of tsunami lies in the upheaved region. In the case of the Niigata earthquake, the amount of upheaval at the sea bottom was about 5 m. The source area shown in Fig. 11 would be extended to the north along the coast, if the tsunami source inferred from an inverse refraction diagram is taken into account.

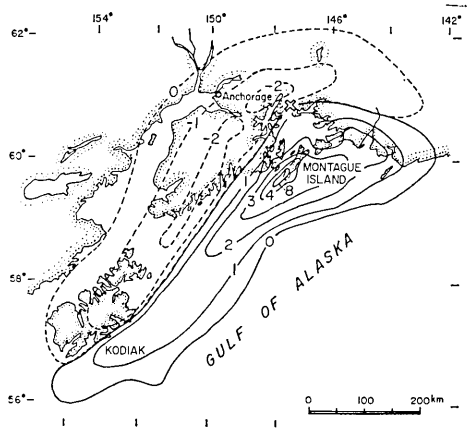

Fig. 10. Contours of vertical crustal deformation, in meters, for the 1964 Alaska earthquake (after G. Plafkea).

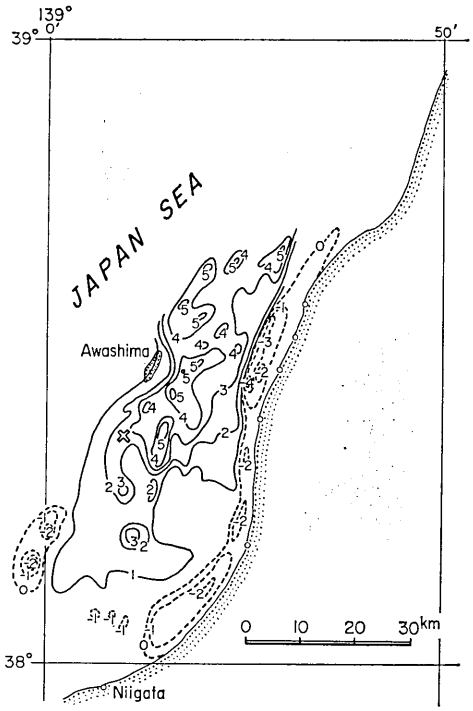

Fig. 11. Contours of vertical deformation on the sea bottom, in meters, for the 1964 Niigata earthquake (after A. Mogi *et al*).

Table 2. Calculated volumes of upheaval and subsidence.

Earthquake	Upheaval Q_u (km³)	Subsidence Q_d (km³)	Remark (km³)
1923 Kanto*	20.2	3.2	
1927 Tango	0.21	0.5	Land: $Q_u=0.03$ $Q_d=0.06$
			Sea: $Q_u=0.18$ $Q_d=0.44$
1935 Taiwan	0.09	0.21	
1935 Oga*	0.04	0.0006	
1943 Tottori	0.003	0.03	
1945 Mikawa	0.1	0.08	Land: $Q_u=0.04$ $Q_d=0.06$
			Sea: $Q_u=0.06$ $Q_d=0.02$
1948 Fukui	0.03	0.07	
1964 Alaska	155	116	
1964 Niigata	4.6	0.4	

* Volume of the displaced material at the land region.

The areas at each interval of the contour lines measured by a planimeter are given in the appendix Tables 1~9. The total volumes of upheaval and subsidence are shown in Table 2. Fig. 12 shows the relation between the upheaved volume and the subsided one plotted on a log-log graph paper. As seen in Fig. 12, in the case of the Tottori earthquake, the subsided volume is remarkably larger than the upheaved one while for the Niigata earthquake it is contrary.

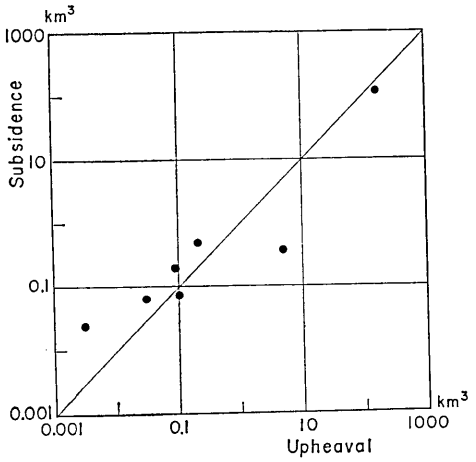

Fig. 12. Relation between the volumes of upheaval and subsidence.

3. Potential energy of tsunami

For the abrupt movement of the submarine crust at the time of earthquake occurrence, the potential tsunami energy can be expressed as follows:

$$E_t = \frac{1}{2}\rho g(Z_1^2 S_1 + Z_2^2 S_2 + \cdots) ,$$

where S is the area at the contour interval, Z the vertical displacement at the contour interval and the density of water is taken as $\rho=1$. If the crustal movement observed on land were transferred to the sea bottom, it would generated tsunami. Thus, the potential tsunami energy could be calculated by the above formula. The calculated values are shown in Table 3. Of course, the values calculated for the sea region represent the real tsunami energy. For the cases listed in Table 4 when the leveling survey was carried out only on a single route, the imaginary tsunami energy was calculated assuming the displaced form on the ground surface as a cone or a disk.

On the other hand, the energy of many tsunamis has been cal-

Table 3. Potential tsunami energy calculated by the present method.

Earthquake	Land region E^* ergs	Sea region E_t ergs	Tsunami energy* E_t ergs
1923 Kanto	1×10^{20}		2.1×10^{20} (Hatori)
			16×10^{20} (Iida, 1963)
1927 Tango	0.8×10^{18}	6×10^{19}	
1935 Taiwan	5×10^{18}		
1939 Oga	0.3×10^{18}		4×10^{18} (Hatori, 1966)
1943 Tottori	1.4×10^{17}		
1945 Mikawa	2.6×10^{18}	3.4×10^{18}	
1948 Fukui	1.4×10^{18}		
1964 Alaska	0.6×10^{22}	1.4×10^{22}	2.3×10^{21} (Van Dorn, 1964)
	(Subsided region)	(Upheaved region)	6×10^{21} (Pararas-Carayannis, 1967)
1964 Niigata		6×10^{20}	0.8×10^{20} (Soloviev et al, 1967)
			2×10^{21} (Hatori, 1966)
			$2\sim10\times10^{21}$ (Iida, 1967)

E^* Imaginary tsunami energy at the land region.
* Calculated value obtained from other methods.

Table 4. Land earthquakes accompanied by crustal deformation and the imaginary tsunami energy (E^*).

Earthquake	M	Upheaval		Subsidence		Calculated volume (km^3)	E^* $\times10^{15}$ ergs
		Displ. (cm)	Length (km)	Displ. (cm)	Length (km)		
1918 Omachi	6.1	20	10			0.005	25
1927 Sekihara	5.3	2.4	6			0.0002	0.14
1949 Imaichi	6.7	5	36			0.01	12
1955 Futatsui	5.7	8	10	5.5	6	0.003	5
1961 Nagaoka	5.2	4	4	2	4	0.0002	0.2
1961 Kita-Mino	7.0	3	44	7	6	0.04	50
1962 N. Miyagi	6.5	3	14	3	4	0.005	7

culated, based on tsunami waves as listed in Table 5*. The tsunami energy obtained from tsunami waves (open circle) and those by the present method (closed circle) are plotted against earthquake magnitude in Fig. 13. The triangles in Fig. 13 are the values of the Kanto** and Oga earthquakes, counting the tsunami energy in the regions of sea and

* Besides, Soloviev and Go (1969) tabled tsunami energies which were calculated by means of a simple supposition.

** Tsunami energy for the Kanto earthquake is calculated, making use of the records observed at tide stations of Ayukawa, Owase and Kushimoto.

Table 5. Tsunami energy obtained from tsunami waves by various investigators.

Date	Location	M	Tsunami energy $E_t \times 10^{22}$ ergs
1928 May 27	Iwate	7.0	0.007 (Hatori, 1966)
1933 Mar. 3	Sanriku	8.3	15 (Watanabe, 1964) 16 (Takahasi, 1951) 17 (Iida, 1963)
1933 June 19	Miyagi	7.1	0.007 (Hatori, 1966)
1936 Nov. 3	〃	7.7	0.2 (Iida, 1963)
1938 May 23	Ibaraki	7.1	0.04 (Iida, 1963)
1938 Nov. 5	〃	7.7	0.2 (Iida, 1963)
1938 Nov. 5	〃	7.6	0.074 (Hatori, 1966)
1938 Nov. 6	Fukushima	7.5	0.027 (Hatori, 1966)
1940 Aug. 2	Shakotan	7.0	0.03 (Hatori, 1966)
1944 Dec. 7	Tonankai	8.0	7.9 (Iida, 1963) 8.8 (Takahasi, 1951)
1945 Feb. 10	Aomori	7.3	0.04 (Iida, 1963)
1946 Dec. 21	Nankaido	8.1	7.2 (Takahasi, 1951) 8.0 (Iida, 1963)
1952 Mar. 4	Tokachi-oki	8.1	3 (Yoshida et al, 1952) 4 (Watanabe, 1964) 8 (Iida, 1963)
1952 Nov. 4	Kamchatka	8.2	14 (Watanabe, 1964) 15 (Iida, 1963)
1953 Nov. 26	Boso-oki	7.5	0.14 (Watanabe, 1964) 0.7 (Iida, 1963)
1957 Mar. 9	Aleutian	8.0	2.7 (Van Dorn, 1963)*
1958 Nov. 6	Iturup	8.2	0.9 (Watanabe, 1964)
1960 Mar. 21	Iwate	7.5	0.4 (Watanabe, 1964) 0.5 (Iida, 1963)
1960 May 22	Chile	8.5	30 (Hirono, 1961), (Miller et al, 1962)* 45 (Iida, 1963)
1961 Feb. 27	Hiuganada	7.0	0.007 (Hatori, 1966)
1963 Oct. 13	Iturup	8.1	1.2 (Hatori, 1966)
1964 May 7	W. Aomori	6.9	0.003 (Hatori, 1966)
1968 May 16	Tokachi-oki	7.9	0.4 (Aida, 1969)** 2.8 (Kishi, 1969)

* Tsunami energy was calculated from decay of waves.
** By method of numerical experiment.

land. As shown in Fig. 13, the values calculated from tsunami waves are larger than those estimated by the present method. However, it may be possible that the values obtained from tsunami waves are overestimated owing to the number of sampled waves. In contrast, the values calculated by the present method have a tendency to be smaller because the surveyed regions did not cover the whole areas of the crustal movement. The comparison of the tsunami energy by the present method with those by other methods is shown in Table 3. For example, in the case of the Niigata tsunami, the energy obtained from tsunami waves is about three times as large as that by the present method.

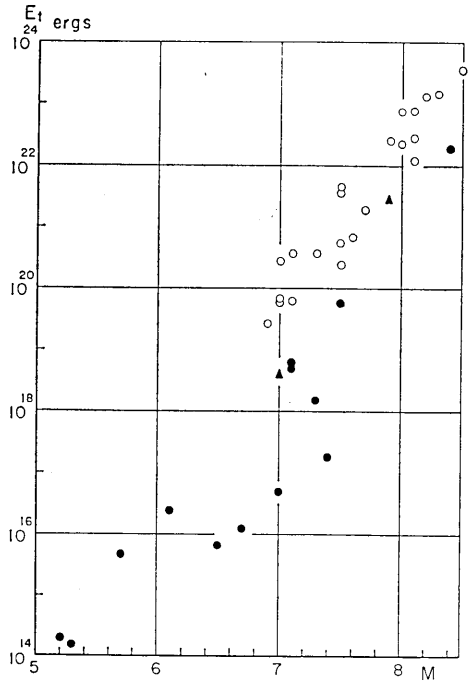

Fig. 13. Relation between tsunami energy and earthquake magnitude. Closed circle: the imaginary tsunami energy calculated from the vertical displacement of the ground caused by land earthquake, open circle: tsunami energy which was calculated on the basis of tsunami waves.

4. Conclusion

On the assumption that a tsunami is generated by land earthquake, the potential tsunami energy is calculated, making use of the surveyed data of the crustal movement. Generally speaking, the tsunami energy calculated by the present method is smaller than that inferred on the basis of tsunami waves. The reason for this discrepancy is not clear at present. The overestimation of the energy by the wave method, and the underestimation of the energy by the present method would both contribute to this discrepancy. The real difference between the magnitude of the crustal deformation on land and in the sea might also be present.

Acknowledgements

The author wishes to express his heartfelt thanks to Prof. K. Kajiura for his valuable advice. His thanks are also due to Mr. M. Koyama who has assisted in the measurement of the areas using a planimeter.

Appendix (Tables 1–9)

Table 1. Areas at each range of vertical displacement at the land region for the 1923 Kanto earthquake.

Upheaval

Displ. (m)	0	0–0.4	0.4	0.4–1.0	1.0–1.4	1.4
Area ($\times 10^2$ km^2)	33.24	14.96	0.13	9.88	5.93	2.34

Subsidence

Displ. (m)	0.6	0.6–1	1
Area ($\times 10^2$ km^2)	3.85	3.50	0.35

Table 2. Areas at each range of vertical displacement at the regions of land and sea bottom for the 1927 Tango earthquake.

LAND Upheaval

Displ. (m)	0.1	0.1–0.2	0.2–0.3	0.3	0.4
Area ($\times 10^2$ km^2)	1.27	0.55	0.29	0.36	0.07

Subsidence

Displ. (m)	0.1	0.1–0.2	0.2–0.3	0.3
Area ($\times 10^2$ km^2)	33.1	2.55	0.68	0.08

SEA Upheaval

Displ. (m)	1	1–2	2	4
Area ($\times 10^2$ km^2)	1.00	0.45	0.1	0.02

Subsidence

Displ. (m)	1	1–2	2	2–3	3	4	5
Area ($\times 10^2$ km^2)	0.34	1.18	0.51	0.29	0.15	0.05	0.03

Table 3. Areas at each range of vertical displacement for the 1935 Taiwan earthquake.

Upheaval

Displ. (m)	0.1	0.1-0.2	0.2	0.3	0.5	0.5-1.0	1.0
Area ($\times 10^2$ km^2)	1.04	1.85	0.21	0.08	0.32	0.1	0.09

Subsidence

Displ. (m)	0.1-0.2	0.2	0.2-0.4	0.4	0.4-0.5	0.5	1.2
Area ($\times 10^2$ km^2)	3.57	1.90	1.51	0.19	0.81	0.46	0.07

Table 4. Areas at each range of vertical displacement at the land region for the 1939 Oga earthquake.

Upheaval

Displ. (cm)	0	0-5	5	5-10	10	10-20	20-40	40
Area ($\times 10^2$ km^2)	6.93	3.52	2.04	0.43	0.15	0.43	0.27	0.09

Subsidence

Displ. (cm)	5
Area ($\times 10^2$ km^2)	0.12

Table 5. Areas at each range of vertical displacement for the 1943 Tottori earthquake.

Upheaval

Displ. (cm)	2	2-4	4-6	6-8	8
Area ($\times 10^2$ km^2)	0.53	0.23	0.19	0.08	0.03

Subsidence

Displ. (cm)	2	2-4	4-6	6	6-8	8-10	10-12	12
Area ($\times 10^2$ km^2)	4.23	1.50	1.44	0.1	0.26	0.14	0.15	0.01

Subsidence

Displ. (cm)	12-14	14-16	16-18	18
Area ($\times 10^2$ km^2)	0.37	0.07	0.13	0.19

Table 6. Areas at each range of vertical displacement at the regions of land and sea bottom for the 1945 Mikawa earthquake.

LAND Upheaval

Displ. (m)	0	0-0.25	0.25-0.5	0.5-0.75	0.75-1.0	1.0-1.25	1.25-1.5	1.5
Area (km^2)	60.6	12.3	12.9	11.6	9.6	12.2	1.7	0.3

Subsidence

Displ. (m)	0.25	0.25-0.5	0.5
Area (km^2)	9.0	147.8	18.0

SEA Upheaval

Displ. (m)	0.3	0.3-0.6	0.6	0.6-0.9	0.9	0.9-1.2	1.2	1.2-1.5	1.5
Area (km^2)	63.7	9.7	1.7	24.2	1.4	15.0	0.6	9.6	1.5

Subsidence

Displ. (m)	0.3	0.3-0.6	0.6	0.6-0.9	0.9
Area (km^2)	1.2	36.8	0.2	9.8	0.2

Table 7. Areas at each range of vertical displacement for the 1948 Fukui earthquake.

Upheaval

Displ. (cm)	0	0-20	20-40	40
Area ($\times 10^2$ km^2)	1.82	1.16	0.58	0.08

Subsidence

Displ. (cm)	0	0-20	20-40	40	40-60	60-80	80
Area ($\times 10^2$ km^2)	2.42	0.96	0.86	0.04	0.34	0.2	0.02

Table 8. Areas at each range of vertical displacement for the 1964 Alaska earthquake.

Upheaval

Displ. (m)	0	0-1	1-2	2-3	3-4	4-8	8
Area ($\times 10^3$ km^2)	105.6	42.6	38.8	14.8	7.7	1.3	0.4

Subsidence

Displ. (m)	0	0-1	1-2	2
Area ($\times 10^3$ km^2)	120.3	68.5	43.0	8.8

Table 9. Areas at each range of vertical displacement on the sea bottom for the 1964 Niigata earthquake.

Upheaval

Displ. (m)	1	1-2	2-3	3-4	4-5	5
Area ($\times 10^2$ km^2)	20*	8*	5*	5.7	1.6	0.1

Subsidence

Displ. (m)	0	0-1	1-2	2
Area ($\times 10^2$ km^2)	4.4	2.6	1.7	0.1

* The area is measured into account the information of the tsunami source.

References

(1) *Crustal deformations*

DAMBARA, T., 1966, Vertical movements of earth's crust in relation to the Matsushiro earthquake (in Japanese), *J. Geodetic Soc. Japan*, **12**, 18-45.

IMAMURA, A., 1941, Land deformations, which accompanied the Oga earthquake of 1939 (in Japanese), *Zisin*, **13** (7), 207-215.

MATUZAWA, T., 1964, *Study of earthquakes*, Uno Shoten, Tokyo, pp. 15-27.

MILITARY LAND SURVEY, 1927, First report on the precise leveling across the province of Tango (in Japanese), *Bull. Earthq. Res. Inst.*, **3**, 167-170.

MILITARY LAND SURVEY, *Reports of leveling and triangulation surveys in the earthquake zone of Taiwan* (in Japanese), Apr. 1937.

MILITARY LAND SURVEY, 1944, Reports of the precise leveling in the Tottori district carried out after the earthquake of 1943 (in Japanese), *Bull. Earthq. Res. Inst.*, **22**, 83-87.

MOGI, A., KAWAMURA, B., and Y. IWABUCHI, 1964, Submarine crustal movement due to the Niigata earthquake in 1964, in the environs of the Awa Island, Japan Sea, *J.*

Geodetic Soc. Japan, **10**, 180-186.

NASU, N., and T. RIKITAKE, 1950, The Fukui earthquake of June 28, 1948, Chapter V. Crustal deformations, *Rep. Fukui Earthq. Comm. Tokyo*, 93-130.

OKADA, A., 1962, Some investigations on the character of crustal deformation, *Bull. Earthq. Res. Inst.*, **40**, 431-493.

PLAFKER, G., 1965, Tectonic deformation associated with the 1964 Alaska earthquake, *Science*, **148** (3678), 1675-1687.

TANAKADATE, H., 1927, Vertical movements at the coast associated with the 1927 Tango earthquake (in Japanese), *J. Geography*, **39**, 617-627, 704-717.

TAYAMA, R., 1949, Geomorphological, geological study of the change of the sea bottom in Atumi Wan (in Japanese), *Hydrogr. Bull.*, **12**, 39-46.

UTIDA, T., 1925, Topographical change of the sea-bottom of Sagami Bay and its vicinity (in Japanese), *Rep. Imperial Earthq. Inv. Comm.*, No. **100**, **B**, 61-62.

YONEMURA, S., 1928, Report of the results soundings in the region off the coast of the Tango province, after the earthquakes of 1927 (in Japanese), *Bull. Earthq. Res. Inst.*, **4**, 227-230.

(*2*) *Tsunami energy*

AIDA, I., 1969, Numerical experiments for the tsunami propagation—the 1964 Niigata tsunami and the 1968 Tokachi-oki tsunami, *Bull. Earthq. Res. Inst.*, **47**, 175-203.

HATORI, T., 1966, Vertical displacement in a tsunami source area and the topography of the sea bottom, *Bull. Earthq. Res. Inst.*, **44**, 1449-1464.

HIRONO, T., 1961, A summary report on the Chilean tsunami (in Japanese), *Tech. Rep. Japan Meteorol. Agency*, **8**, 2-5.

IIDA, K., 1963, A relation of earthquake energy to tsunami energy and the estimation of the vertical displacement in a tsunami source, *J. Earth Sci., Nagoya Univ.*, **11**, 49-67.

IIDA, K., 1967, The Niigata tsunami of June 16, 1964, *Gener. Rep. Niigata Earthq. 1964, Tokyo Electrical Engr. Coll. Press*, 97-127.

KISHI, T., 1969, Tsunami report, May 16, 1968, on the coast of Hokkaido and Tohoku (in Japanese), *Report on the Tokachi-oki Earthq. 1968, Special Comm. Invest. Tokachi-oki Earthq. 1968, Sapporo*, 207-256.

MILLER, G. R. MUNK, W. H., and F. E. SNODGRASS, 1962, Long-period waves over California's continental borderland, Part 2, Tsunamis, *J. Marine Res.*, **20**, 31-41.

PARARAS-CARAYANNIS, G , 1967, A study of the source mechanism of the Alaska earthquake and tsunami of March 27, 1964, Part 1, Water waves, *Pacific Science*, **21**, 301-310.

Соловьев, С. Л., и А. Н. Милитеев, 1967, Динамическая характеристика Ниигатского цунами 1964 г., *Океанология, АН. СССР*, **7**, 104-115.

Соловьев, С. Л., и Ч. Н. Го, 1969, Каталог Цунами в Тихом океане, *АН. СССР, Москва*, 1-83.

TAKAHASI, R., 1951, An estimate of future tsunami damage along the Pacific coast of Japan, *Bull. Earthq. Res. Inst.*, **29**, 71-95.

VAN DORN, W G., 1963, The source motion of the tsunami of March 9, 1957 as deduced from wave measurements at Wake Island, *Pacific Science Congress Symposium, 1961, IUGG Monograph* No. **24**, 39-48.

VAN DORN, W. G., 1964, Source mechanism of the tsunami of March 28, 1964 in Alaska, *Proc. Ninth Conference on Coastal Engineering, Am. Soc. Civil Engr.*, 166-190.

WATANABE, H., 1964, Studies on the tsunamis on the Sanriku coast of the northeastern Honshu in Japan, *Geophy. Mag.*, **32**, 1-64.

YOSHIDA, K., KAJIURA, K., and H. MIYOSHI, 1952, On the tsunami of March 4, 1952, *Geophys. Notes*, **6**, 1-6.

(*3*) *Others*

AIDA, I., 1970, A numerical experiment for the tsunami accompanying the Kanto earth-

quake of 1923 (in Japanese), *Bull. Earthq. Res. Inst.*, **48**, 73-86.
INOUYE, W., 1950, On the Mikawa earthquake of January 13, 1945 (in Japanese), *Quart. J. Seismol.*, **14**, 49-55.
ISHIMOTO, M., 1937, Aftershock occurring and crustal deformation (in Japanese), *Zisin*, **9**, 108-117.
KISHINOUYE, F., and K. IIDA, 1939, The tsunami that accompanied the Oga earthquake of May 1, 1939, *Bull. Earthq. Res. Inst.*, **17**, 733-740.
MIYOSHI, H., 1968, Bottom deformation and energy of tsunami, 1 (in Japanese), *Zisin*, [ii], **21**, 72-74.
MOGI, A., 1959, On the depth change at the time of Kanto-Earthquake in Sagami Bay (in Japanese), *Hydrogr. Bull.*, **60**, 52-60.

---

12. 地殻の上下変動と津波のエネルギー

地震研究所　羽鳥徳太郎

1933年三陸津波について，波源に近い沿岸で測られた津波の振幅と周期から，津波エネルギーの推定が高橋 (1951) によつて初めて試みられた．その後検潮記録をもとに，多くの研究者によつて多数の津波のエネルギーが計算されてきた．しかし津波によつては，1桁も計算値に幅があつた．今回，これら津波波形から得られた津波エネルギーを検討する一つの手段として，次のようなことを行なう．すなわち沿岸で海底変動を伴つた地震を含め，陸上の地震でも津波が起こつたと想定し，地震による地表の上下変動の形を，そのまま水位の変化とみなして，仮想の津波のポテンシャル・エネルギーを計算した．

なお，地震の前後に測地が行なわれた1927年丹後，1943年鳥取，1948年福井地震では，水準・三角点の上下変動値を基準として等高線を画く操作を行ない，等高線の間隔ごとの面積をプラニメーターで測り，変動の体積を求めた．また一つの水準路線上で測地が行なわれた地震も，解析の資料としてとり上げている．

今回の方法で得た計算値と，津波の波形から求められた津波のエネルギーを地震の規模に対して比較すると，海の地震の方が陸の地震よりもエネルギーが大きいという，傾向が認められる．しかし波形から求められた津波エネルギーは，波数のきめ方に問題があつて（高橋によると，計算には3山と2谷の波が使われている），エネルギーは過大に見積られるように思われる．一方，陸上の地震では，測地が変動域を十分に行なわれない場合もあつて，計算値は過小評価されることが考えられる．例えば1964年新潟地震では，津波の波形から求められた津波エネルギーは，今回得たものより約3倍大きく推定された．

以上のように，測地ならびに計算の誤差が伴つて，地域差についての結論は速かにきめられないが，地震の規模に対する津波エネルギーのオーダーを推測することができた．また数個の地震については，隆起と沈降量との比較を参考までに示す．